Effect of geometrical frustration on the magnetic properties of the triangular-layer system $Tb_2C_2I_2$: a neutron diffraction investigation

2004 J. Phys.: Condens. Matter 16 S875

(http://iopscience.iop.org/0953-8984/16/11/043)

INSTITUTE OF PHYSICS PUBLISHING JOURNAL OF PHYSICS: CONDENSED MATTER

J. Phys.: Condens. Matter **16** (2004) S875–S881 PII: S0953-8984(04)74114-4

Effect of geometrical frustration on the magnetic properties of the triangular-layer system $Tb_2C_2I_2$: a neutron diffraction investigation

Kyungsoo Ahn[1], **Reinhard K Kremer and Arndt Simon**

Max-Planck-Institut für Festkörperforschung, Heisenbergstrasse 1, D-70569 Stuttgart, Germany

Received 7 January 2004
Published 4 March 2004
Online at stacks.iop.org/JPhysCM/16/S875 (DOI: 10.1088/0953-8984/16/11/043)

Abstract

Powder neutron diffraction on $Tb_2C_2I_2$ reveals strong resolution-limited magnetic Bragg reflections below 60 K due to commensurate antiferromagnetic (afm) long range ordering. Between 60 and 85 K the magnetic reflections broaden beyond instrumental resolution and the propagation vector becomes incommensurate. Above ≈95 K magnetic scattering is only seen as a diffuse ridge which we ascribe to short-range correlations within the triangular Tb atom planes. With decreasing temperature an additional Lorentzian shaped reflection grows on top of the decaying edge of this diffuse ridge. We analyse the diffuse scattering by fitting a Warren-type lineshape and a Lorentzian shaped Bragg reflection. The results of the fits indicate that, with diverging intra-plane correlations, significant inter-plane afm correlations build up close to 85 K. Above 95 K inter-plane correlations are essentially limited to nearest-neighbour Tb atom double layers only.

1. Introduction

Magnetic ordering on layered triangular lattices with antiferromagnetic (afm) coupling is governed by *geometrical frustration* effects. For example, ordering on a nearest-neighbour afm coupled triangular lattice is frustrated because at least one afm bond on each triangle must be broken, viz the moments must be parallel instead of antiparallel. Wannier, in his pioneering work, demonstrated that the two-dimensional nearest-neighbour afm Ising model on an isotropic triangular lattice does not undergo long-range order and the entropy rather remains finite at absolute zero [1]. In a real structure containing triangular layers, long range ordering in general emerges from inter-layer coupling. The investigation of the properties of systems containing triangular afm coupled layers is well known in magnetism and has proven rewarding for testing theories for cooperative phenomena and for spotting magnetic systems with unusual ground state properties (see, e.g., [2]).

[1] New address: Department of Chemistry, Yonsei University, Wonju, Korea.

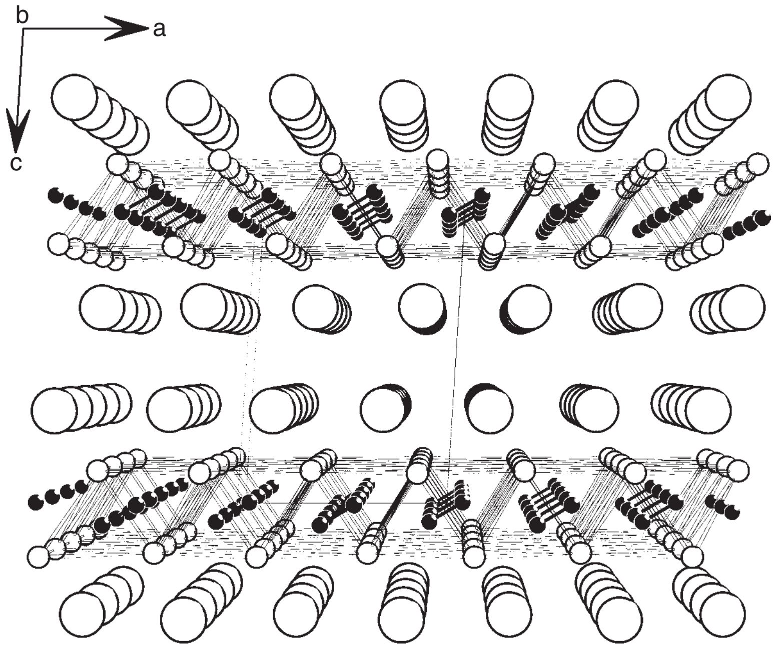

Figure 1. Perspective view along [010] of the crystal structures of $Tb_2C_2I_2$ with a unit cell outlined. The distance between adjacent double layers amounts to 10.4 Å.

Here, we present a neutron diffraction investigation of the magnetic diffuse scattering of the system $Tb_2C_2I_2$ which contains triangular layers of magnetic Tb ions. In the crystal structure of $Tb_2C_2I_2$ two such (distorted) triangular layers combine to build a close packed double layer with C_2 dumbbell units occupying the octahedral metal atom voids. The double layers are sandwiched by layers of halogen atoms to form I–Tb–C_2–Tb–I slabs which connect via van der Waals forces in stacks along the crystallographic *c* axis (cf figure 1). Our interest in the layered rare earth carbide halides containing magnetic rare earth elements has been triggered by the observation of superconductivity up to $\approx$12 K in the isostructural Y and La layered carbide halides [3–5].

In a previous neutron powder diffraction study, $Tb_2C_2I_2$ was found to exhibit long range afm order below $\approx$60 K, but with an unusual ordering feature preceding the Néel point. These features are evident, for example, in the magnetic susceptibility, the heat capacity and the electrical resistivity [6]. We attribute them to the pronounced anisotropic structure with strong magnetic coupling within the layers and weaker superexchange coupling via halogen atoms between them.

The afm ordering temperature of $\approx$60 K of $Tb_2C_2I_2$ in fact is very close to the Néel temperature of the binary carbide TbC_2 (66 K) crystallizing in the CaC_2 structure type [7]. This coincidence may indicate a close electronic and magnetic bonding similarity of the Tb–C_2–Tb double layers with that in the three-dimensionally connected Tb–C network in TbC_2.

2. Experimental details and data treatment

Polycrystalline samples of $Tb_2C_2I_2$ were synthesized from Tb metal, TbI_3 and carbon powder. Sample preparation and handling of the moisture-sensitive samples are described in detail elsewhere [6]. The products were characterized with x-ray and neutron powder diffraction.

Neutron patterns at room temperature were collected on ILL's powder diffractometers D2B ($\lambda = 1.594$ Å) and between ≈2 and 130 K on D20 ($\lambda = 2.41$ Å) from a polycrystalline sample of about 5 g which was encapsulated in a thin-walled vanadium container filled with dried He at 1 bar [8]. Neutron powder diffraction at variable temperatures was performed while slowly heating the sample from ≈2 up to 130 K. Rietveld profile refinement of the D2B powder patterns was carried out using the program Mac-Rietan [9]. The magnetic susceptibility of a crystal (≈300 μg) selected from the polycrystalline sample used for neutron diffraction was determined with a MPMS7 magnetometer (Quantum Design). The crystal was mounted in a carefully vacuum annealed quartz glass ampoule under a He atmosphere such that the external field was oriented within the *ab* plane.

For a quantitative analysis of the diffuse magnetic scattering we used difference patterns obtained after subtracting the 125 K pattern from the individual patterns collected at lower temperature. Difference patterns were used to avoid deterioration of the weak diffuse scattering by nearby significantly more intense nuclear Bragg reflections.

The magnetic diffuse scattering between $10° \leqslant 2\theta \leqslant 30°$, $I_{mag}(\theta)$, was analysed by fitting it to a superposition of a Warren-type lineshape, $I_W(2\theta)$, and a Lorentzian broadened magnetic Bragg reflection, $I_L(2\theta)$. In addition, we included a constant background A and allowed for a linear variation of the background with $B2\theta$:

$$I_{mag}(2\theta) = I_W(2\theta) + I_L(2\theta) + A + B2\theta. \tag{1}$$

$I_W(2\theta)$ was calculated adopting the standard expression given by Warren for layered lattice structures with finite particle size within the layers stacked along a perpendicular axis [10]:

$$I_W(2\theta) = I_{W0} f^2(Q) \frac{1 + \cos^2(2\theta)}{2(\sin(\theta))^{3/2}} \left(\frac{L_{intra}}{\sqrt{\pi}\lambda}\right)^{1/2} F(a) \tag{2}$$

wherein I_{W0} is the relative intensity and $f(Q)$ is the magnetic form factor at wavevector Q taken for Tb^{3+} from [11]. The variable $a = 2\sqrt{\pi} L_{intra}/\lambda(\sin(\theta) - \sin(\theta_{W0}))$ is essentially determined by the ratio of the *particle dimension* L_{intra} to the neutron wavelength λ. θ_{W0} is the peak position of the Warren line. We identify the characteristic extension of intra-plane short-range magnetically correlated regions with L_{intra}. $F(a)$ is defined in [10]. $F(a)$ was calculated by standard numerical integration routines. The inter-plane correlation length, L_{inter}, was estimated from the width of the broadened inter-plane Bragg reflection determined from a Lorentzian profile fit according to

$$I_L(2\theta) = I_{L0} \frac{2\pi}{\Delta\theta_L} \frac{1}{1 + x^2} \tag{3}$$

with $x = 2(\theta - \theta_{L0})/\Delta\theta_L$, $\Delta\theta_L$ is the full width at half-maximum (FWHM) and θ_{L0} the position of the Lorentzian shaped Bragg reflection. L_{inter} was estimated from $\Delta\theta_L$ using Scherrer's particle size equation [12]:

$$L_{inter} = \frac{0.94}{\cos(\theta_{L0})} \frac{\lambda}{\Delta\theta_L}. \tag{4}$$

Finite instrumental resolution was taken into account by allowing a Gaussian *smearing* of θ_{W0} and θ_{L0}. The width of this Gaussian was taken from the width of the resolution-limited magnetic Bragg reflections of the long range ordered afm phase at ≈2 K in the respective 2θ range.

3. Results and discussion

Rietveld refinements of the high resolution powder diffraction patterns collected at D2B proved the phase purity of our sample. All reflections can be indexed on the basis of the structure

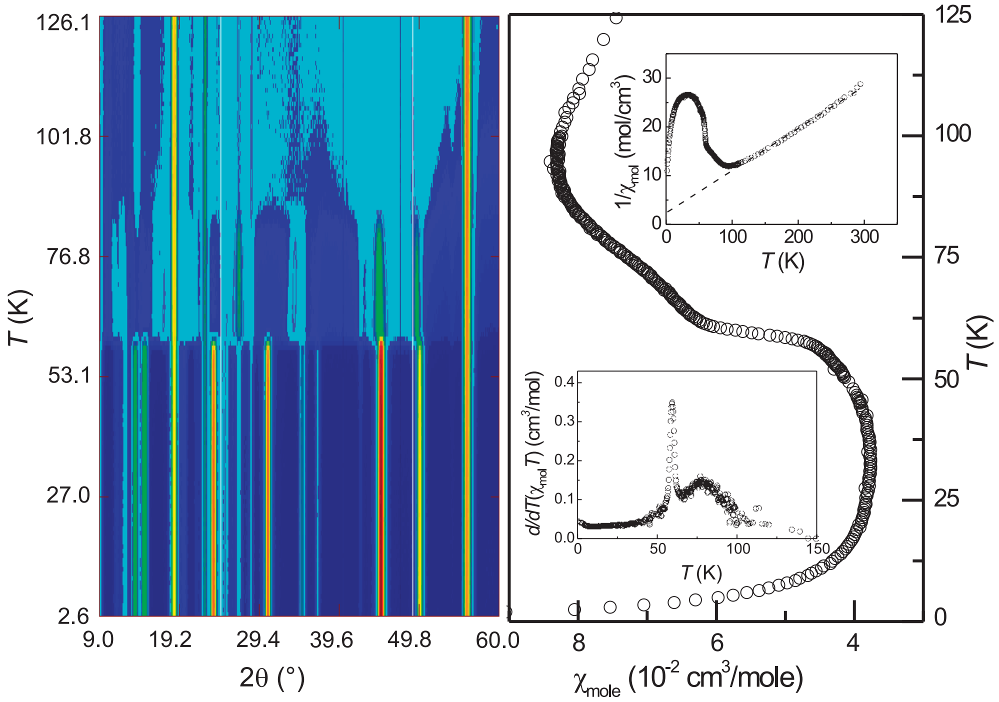

Figure 2. Left: thermodiffractogram (false colour representation) of 1s-$Tb_2C_2I_2$ taken at the powder diffractometer D20 (ILL, Grenoble, France). Yellow and red colours mark zones of high intensity (coherent nuclear and magnetic Bragg reflections). A light blue colour indicates weak diffuse magnetic scattering above ≈85 K. A wavelength of $\lambda = 2.4$ Å was used in all measurements. Right: magnetic susceptibility, inverse magnetic susceptibility and Fisher's heat capacity, $d/dT(\chi_{mol}T)$ (insets) of a crystal (≈330(30) μg) of $Tb_2C_2I_2$ taken from the polycrystalline sample used for powder neutron diffraction experiments. The magnetic field (0.01 T) was oriented in the *ab* plane.

(This figure is in colour only in the electronic version)

established for 1s-$Y_2C_2I_2$ (see figure 1) [13]. The refined atom positional parameters are in close agreement with those reported for $Y_2C_2I_2$ [13]. The refinement of the C occupancy within error bars indicates a stoichiometric phase with an upper limit for the C deficiency of ≈1.4%.

Above 150 K the magnetic susceptibility of the $Tb_2C_2I_2$ crystal follows a Curie–Weiss law with an effective magnetic moment of $\mu_{eff} = 9.5(5)\ \mu_B$, in agreement with the expected effective moment of 9.72 μ_B for Tb^{3+} with its $4f^8$ configuration and $^7F_6$ ground state. The paramagnetic Curie temperature is negative and amounts to −27(3) K, indicating predominant afm exchange. At ≈95 K a broad maximum appears in the susceptibility which we ascribe to afm short range correlations. The edge in the susceptibility at ≈60 K gives rise to a sharp spike in the quantity $d/dT(\chi_{mol}T)$ ('Fishers heat capacity') which marks the onset of commensurate long-range afm ordering (see figure 2 (inset)).

The temperature dependence of the neutron powder diffraction of $Tb_2C_2I_2$ as measured using diffractometer D20 is composed and displayed as a *thermodiffractogram* in figure 2. It reveals two magnetic transitions at about 85 and 60 K, respectively. Below 60 K sharp additional magnetic Bragg reflections due to long range afm ordering are observed. Details of the magnetic structure have been reported previously [6]: the ordered magnetic moment amounts to 8.0(1) μ_B and thus is slightly smaller than the maximum possible moment ($J = 6$,

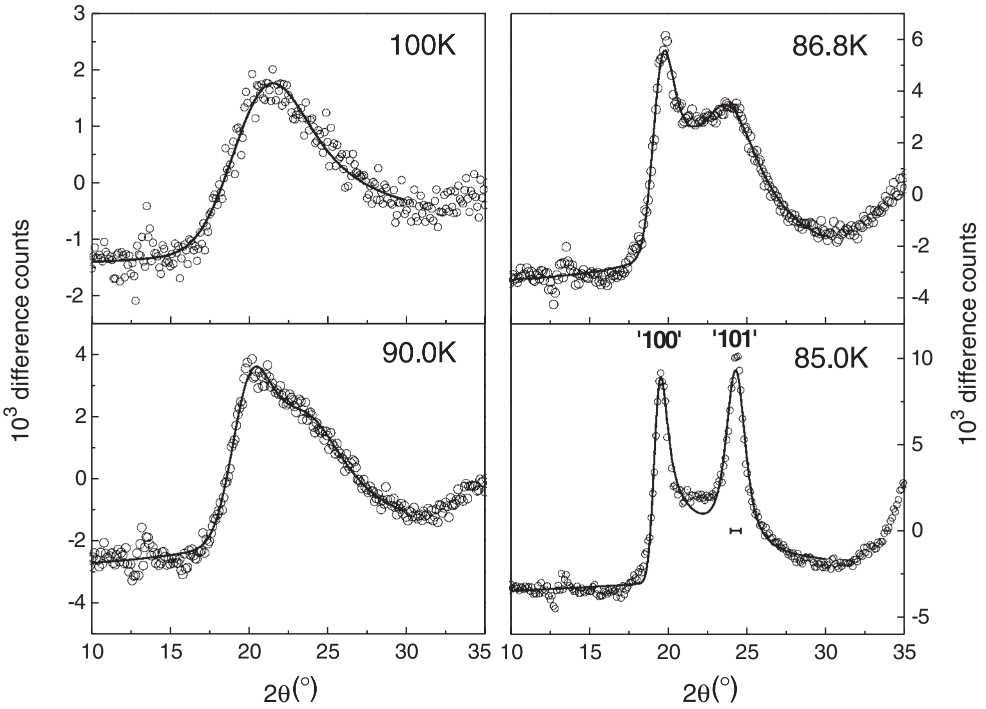

Figure 3. Fit of equation (1) (full curve) to the difference neutron counts (see the text) at the indicated temperatures. The horizontal bar in the 85 K pattern indicates the instrumental resolution. Approximate indices are given for the two reflections.

$g_J = 3/2$) of a Tb^{3+} ion (9 μ_B). The moments were found to lie in the *ac* plane. They point parallel along the *b* axis and antiparallel along the *a* axis. The almost fully developed moment will go along with a significant uniaxial anisotropy and a pronounced anisotropic exchange may be expected.

Between 85 and 60 K the magnetic Bragg reflections broaden beyond experimental resolution and they become incommensurate with the underlying nuclear lattice. The nature of this incommensurate phase could not be solved yet. Above ≈85 K the magnetic reflections decay into a diffuse but structured magnetic background which decreases in intensity with growing temperature. Most pronounced is the diffuse scattering in the angular range $10° \leqslant 2\theta \leqslant 35°$ emerging from the magnetic Bragg reflections 100 and 101. Above 95 K it shows a characteristic Warren lineshape with a steep increase at the low angular edge and an extended concave decay above the maximum. With decreasing temperature, a Lorentzian shaped reflection grows out of the extended decaying part of the Warren profile. This reflection is close to the position of the 101 reflection in the low-temperature commensurate afm phase. It is significantly broader than expected from experimental resolution. Figure 3 displays the results of the fits of equation (1) to the difference patterns at the indicated temperatures. Note the different ordinate scales used to magnify the diffuse intensity towards higher temperatures. The extracted inverse intra-plane correlation length, $\lambda/L_{\mathrm{intra}}$, and the FWHM of the symmetric Lorentzian shaped reflection at $2\theta \approx 24°$, $\Delta\theta_L$, are displayed in figure 4.

The intra-plane correlation length L_{intra} undergoes a continuous transition with a critical temperature $T_C = 86.7(1)$ K as obtained from a fit of a power law assuming a mean-field critical exponent $\nu = 1/2$. Below 90 K, the diverging intra-plane correlations induce a rapid decrease

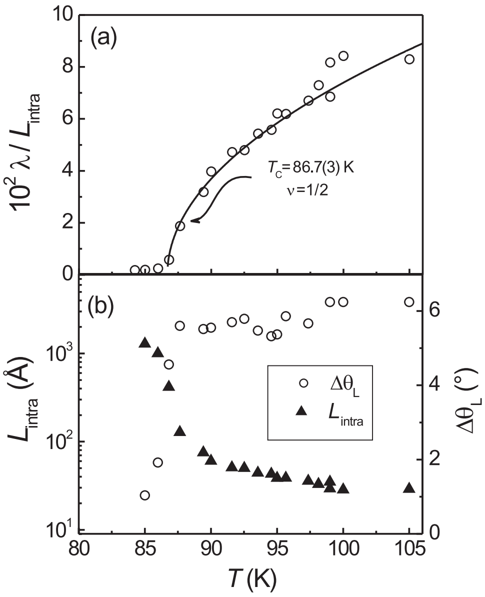

Figure 4. (a) Inverse intra-plane correlation length $\lambda/L_{\rm intra}$ obtained from the fits of a Warren profile ($\lambda = 2.41$ Å). The full curve represents a fit with a power law with critical exponent $\nu = 0.5$. (b) FWHM, $\Delta\theta_{\rm L}$, of the Lorentzian fitted to the magnetic Bragg reflection centred at $2\theta \approx 24°$ ($\approx$101) and derived inter-plane correlation length $L_{\rm inter}$.

of the width of the reflection at $2\theta \approx 24°$. Its FWHM drops in a narrow temperature interval between 88 and 85 K from 6° above 88 K to $\lesssim$1° below 85 K. However, even below 85 K the lineshape is still Lorentzian and the FWHM of $\approx$1° is still significantly above the instrumental resolution ($\approx$0.5°). Between 86.7 and $\approx$60 K this reflection remains incommensurate with the underlying nuclear lattice, but below 60 K changes its position and can be well indexed as 101. We take the width of the '101' reflection as a measure for inter-plane correlations and use equation (4) to convert the width of 1° to a correlation length of about $\approx$7 times the inter-plane distance c. Above 88 K the inter-plane correlation length amounts to only one lattice constant $\approx c$.

In conclusion, the magnetic behaviour of $Tb_2C_2I_2$ above the commensurate afm transition at 60 K can be summarized in the following way: below $\approx$150 K increasing afm short range correlations within the Tb atom double layers develop. These lead to the observed broad maximum in the susceptibility and the characteristic Warren-type diffuse magnetic scattering. First inter-plane correlations start to develop only below $\approx$95 K and they give rise to, for example, a broad incommensurate Bragg reflection close to the position of the 101 reflection. Inter-plane correlations remain at first essentially short-ranged and are confined to $\approx$10 Å or to the nearest-neighbour Tb double layer only. Sizeable inter-plane correlations apparently deserve sufficiently extended intra-plane correlated regions which grow rapidly close to 87 K. While the increase of the intra-plane correlations appears to happen in a continuous phase transition the inter-plane correlations rise sharply within a narrow temperature range, possibly indicating that this transition is discontinuous. Resulting from this transition is an incommensurate phase, the origin of which we ascribe to magnetic frustration of the Tb moments within the triangular layers. The heat capacity displays an anomaly in this temperature range which is, however, considerably broader than the sharp anomaly associated with the incommensurate/commensurate transition at $\approx$60 K.

Ordering in the incommensurate phase is by no means long range. In the incommensurate phase finite correlated regions extend rather to about $\approx$500(50) Å within the Tb layers and $\approx$70 Å across the layers, viz the extension of about seven Tb atom double layers. An explanation for this behaviour must be searched for in the complex interplay of essentially two-dimensional exchange coupled layers together with a pronounced uniaxial single-ion anisotropy (connected by significantly weaker Tb–I–I–Tb inter-layer superexchange only), on the one hand, and the triangular arrangement of the Tb moments imposing a high degree of magnetic frustration on the other hand.

The observed magnetic behaviour of $Tb_2C_2I_2$ is reminiscent of that observed for the layered triangular system $InMnO_3$ analysed by Greedan *et al* [14]. At present, we cannot make a conclusive statement as to whether the intra-plane correlations in the Tb atom double layers extend up to room temperature, as is seen for the Mn layers in $InMnO_3$. However, it appears that, in contrast to $InMnO_3$, intra-plane correlations decay faster with increasing temperature.

Also, in clear contrast to $InMnO_3$, $Tb_2C_2I_2$ shows well developed afm long range ordering at low temperatures with no indication of finite size spin correlations remaining at low temperatures. Long range ordering may be imposed by weak inter-plane superexchange interaction via Tb–I–I–Tb paths. We refer to the discussion of the phase diagrams of the various stacked triangular lattices and the occurrence of incommensurate phases due to inter-plane coupling, as also observed for $Tb_2C_2I_2$ between 60 and 85 K [15]. The occurrence of double layers and their stacking in $Tb_2C_2I_2$ is different from the conventional hexagonal or cubic close packed layer systems. The principles, however, may remain very similar.

Finally, we note that the Tb atom layers are not arranged in perfect triangles and that a resulting anisotropy of the exchange coupling may assist in lifting the degeneracy and lead to long-range ordering as pointed out by Vaks and Geilikman [16]. Additionally, coupling to next-nearest and further distant neighbours due to long range RKKY interactions in the metallic $Tb_2C_2I_2$ may also become important.

Acknowledgments

We thank E Brücher and G Siegle for technical assistance and acknowledge the kind assistance of P Convert and T Hansen from the ILL during the neutron diffraction experiments.

References

[1] Wannier G H 1950 *Phys. Rev.* **79** 357
[2] Ramirez A P 1994 *Annu. Rev. Mater. Sci.* **24** 453
[3] Simon A, Mattausch Hj, Eger R and Kremer R K 1991 *Angew. Chem. Int. Edn Engl.* **30** 1188
[4] Henn R W, Schnelle W, Kremer R K and Simon A 1996 *Phys. Rev. Lett.* **77** 374
[5] Ahn K, Gibson B J, Kremer R K, Mattausch Hj, Stolovits A and Simon A 1999 *J. Phys. Chem.* B **103** 5446
[6] Ahn K, Gibson B J, Kremer R K, Mattausch Hj, Keller L and Simon A 2001 *J. Alloys Compounds* **323/324** 400
[7] Atoji M 1966 *Phys. Lett.* **23** 208
Atoji M 1967 *J. Chem. Phys.* **46** 1891
[8] for details see http://www.ill.fr/YellowBook/D2B/ and http://www.ill.fr/YellowBook/D20/
[9] Izumi F and Ikeda T 2000 *Mater. Sci. Forum* **321–324** 198
[10] Warren B E 1941 *Phys. Rev.* **59** 693
[11] Brown P J 1999 *International Tables for Crystallography* vol C, ed A J C Wilson (Dordrecht: Kluwer) p p 391 ff
[12] Warren B E 1985 *X-Ray Diffraction* (Reading, MA: Addison-Wesley) p p 253
[13] Mattausch Hj, Borrmann H and Simon A 1994 *Z. Kristallogr.* **209** 281
[14] Greedan J E, Bieringer M, Britten J F, Giaquinta D M and zur Loye H-C 1995 *J. Solid State Chem.* **116** 118
[15] Reimers J N and Dahn J R 1992 *J. Phys.: Condens. Matter* **4** 8105
[16] Vaks V G and Geilikman M B 1971 *Sov. Phys.—JETP* **33** 179